

# VESICA: Computer graphics modeling of lipid vesicles

S.M. Lawrence\*, M.J. Lawrence\*, and D.J. Barlow\*†

Departments of Pharmacy\* and Pharmacology†, King's College, University of London, London SW3 6LX, UK

*A vesicle simulation and computer analysis program, VESICA, is described which employs spherical projections of triangularly tessellated icosahedra to produce molecular graphics models of the three-dimensional structures of lipid vesicles. The program is used to analyze the molecular architecture of small unilamellar vesicles of dipalmitoylphosphatidylcholine and is demonstrated as a worthwhile investigative tool for determining the factors that govern the minimum vesicle size.*

**Keywords:** phospholipid vesicles, icosahedral tessellation, drug delivery, lipid bilayer, membranes

## INTRODUCTION

Phospholipid vesicles have been extensively investigated as both model membranes<sup>1</sup> and drug delivery systems;<sup>2</sup> in their applications in drug delivery, however, these systems have yet to prove as valuable as first expected. This is because the vesicles employed are prepared using charged natural phospholipids, which causes them to have low stability and short *in vivo* lifetimes. Since the properties of the vesicles are dictated by their surface characteristics,<sup>3</sup> recent research has been directed toward the development of suitable uncharged systems based on novel nonionic amphiphiles.<sup>4</sup> Ideally, these novel amphiphiles would be tailored to give vesicles with predetermined properties, but this is impossible at present because of our poor understanding of the relationship between lipid and vesicle structures. Although the nature of lipid packing within vesicular bilayers has been modeled on the basis of thermodynamic<sup>5</sup> and simple geometric considerations,<sup>6</sup> there is still a great deal of controversy in this area. There has been very little effort made to study the systems in molecular and atomic detail, and the computer graphics work carried out so far has been limited to planar membranes.<sup>7</sup>

In the following report, a vesicle simulation and computer analysis program, VESICA, is described, which has been developed as a first step toward rectifying this deficiency.

In its present form the program is intended simply as an investigative tool to aid in elucidating the physiochemical principles that dictate a vesicle's molecular architecture. The applications of the program are demonstrated here by modeling small unilamellar vesicles (SUVs) composed of dipalmitoylphosphatidylcholine (DPPC); its applications also extend to modeling other sorts of lipid aggregates, such as spherical micelles, inverted micelles, and micro-emulsions.

Preliminary accounts of this and related work have been reported elsewhere.<sup>8,9</sup>

## METHODS

The four stages involved in VESICA's construction of computer graphics models for lipid vesicles are:

- (1) Calculation of the vesicle and bilayer dimensions
- (2) Generation of monolayer templates for the vesicle bilayer
- (3) Positioning of lipid molecules onto the loci provided by these templates
- (4) Adjustment of the lipid conformations to produce models consistent with experimentally determined dimensions of the vesicle bilayer.

In this section we deal with Stages 2, 3, and 4 and defer the discussion of the calculations involved in Stage 1 until later.

### Construction of monolayer templates

The first task in modeling the three-dimensional (3D) structure of a lipid monolayer is to determine the loci for the monomer polar head groups. In the present study, the lipid molecules are assumed to be hexagonally closed-packed<sup>10</sup> and the desired loci are obtained as spherical projections of triangularly tessellated icosahedra.<sup>11</sup> The general nature of this tessellation is shown in Figures 1 and 2, and the details of its construction and use for modeling the templates of lipid monolayers are summarized below:

- (1) The starting point for all templates is provided by the 12 vertices of a regular icosahedron. The Cartesian coordinates of these vertices (expressed in Å) are initially taken as

$$(0, \pm 1, \pm \tau); (\pm 1, \pm \tau, 0); (\pm \tau, 0, \pm 1)$$

where  $\tau$  is the Golden ratio  $(1 + \sqrt{5})/2$ . The resulting

Address reprint requests to Dr. Barlow at the Department of Pharmacy, King's College, University of London, Manresa Road, London SW3 6LX, UK.

Received 27 November 1990; accepted 12 February 1991

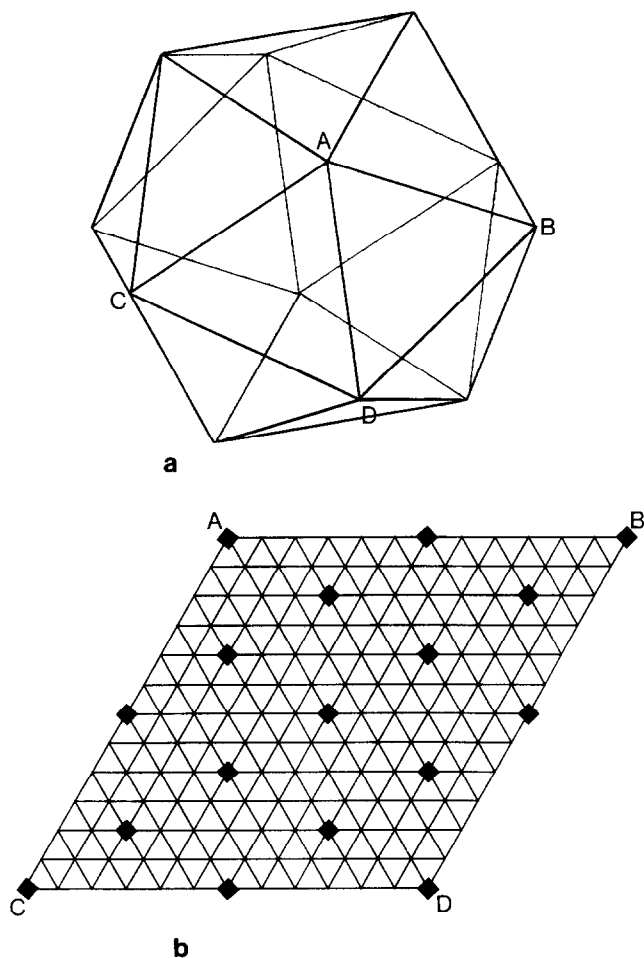


Figure 1. *a*, Basic icosahedron used as the starting point for a lipid monolayer template. The vertices of the two adjacent faces are labeled A to D; *b*, icosahedron rhombus produced by flattening the two icosahedral faces labeled in *a*. The additional points added to the figure provide a tessellation of  $T = 12$ ; when wrapped about an icosahedron, this tessellation gives 4 extra points on each triangular face, and 1 extra on each edge, arranged at the nodes of a lattice 12 times finer. The algorithm employed in construction of the lattice is detailed in the text and in Figures 3 and 4

figure is an icosahedron with edge length  $d = 2 \text{ \AA}$ , and circumsphere radius  $r = 1.902 \text{ \AA}$ .

- (2) To model a spherical monolayer in which the mean distance between the vesicle center and the lipid polar head groups is  $P \text{ \AA}$ , the basic polytope prepared in Step 1 is scaled by a factor  $S$ , where  $S = P/r$ . After scaling, the intervertex separation of the icosahedron is then  $2S \text{ \AA}$ . As a template for a lipid monolayer, therefore, this figure provides sufficient loci for positioning only 12 lipid molecules, each of which will close pack in pentagonal fashion, given that the molecules have a head group radius of  $S \text{ \AA}$ .
- (3) For monolayers with hexagonally close-packed lipids and higher aggregation numbers, it is necessary to add extra vertices to the icosahedron, calculated by an appropriate icosahedral tessellation. The allowed orders

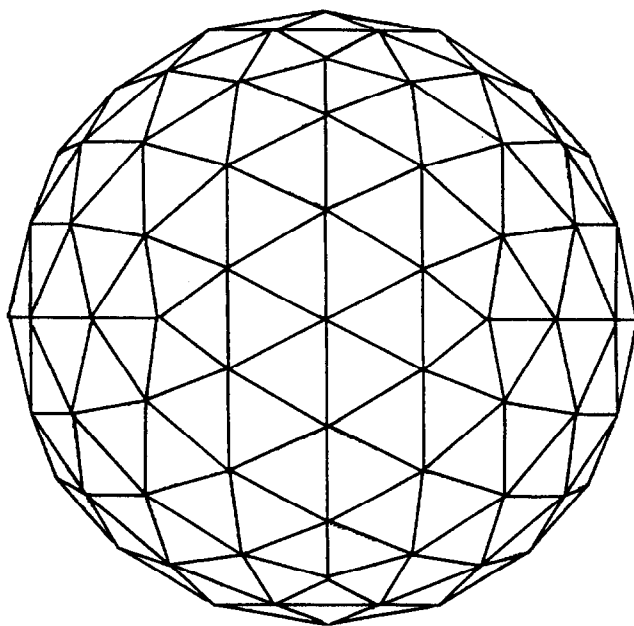


Figure 2. Tessellated icosahedron  $T = 12$  with all vertices normalized to lie at the same distance from its center

of tessellation ( $T$ ) are given by:

$$T = h^2 + hk + k^2 \quad (1)$$

where  $h$  and  $k$  are positive integers. For a given value of  $T$  there will be  $(T - 1)/2$  additional points added to each of the 20 icosahedron faces, giving  $10T + 2$  points in total. The intervertex separation of the tessellated icosahedron is then  $1/\sqrt{T}$  of the original figure.

When constructing the template for a monolayer with an aggregation number  $N$  (that is, one which will accommodate  $N$  lipid molecules), the desired order of tessellation ( $T_d$ ) is obtained as  $(N - 2)/10$ . As will be apparent from Equation (1), however, not all values of  $T$  are admissible, and so the best that can be done is to find the value of  $T$  that gives the closest approximation to  $T_d$ . Unfortunately this task is made nontrivial by the fact that there is no known principle by which the allowed values of  $T$  may be systematically generated in perfect sequence. As a necessary evil, therefore, we have developed the algorithm summarized in Figure 3. In this procedure, the value of  $T$  that is closest to  $T_d$  is determined using the empirical observation that this  $T(T')$  has  $(h + k)$  in the range  $nl$  to  $nu$  where  $nl = \text{INT}[2T^{1/2}/3]$  and  $nu = 2[(nl/2) + 1]$ . All values of  $T$  between these limits are thus produced in imperfect sequence, and the resulting list is scanned for the values that are closest above and below  $T_d$ . The final choice (between these two tessellations) is then left to the user's discretion.

- (4) When the appropriate order of tessellation has been determined, the Cartesian coordinates are generated for the additional lattice points required, using the method illustrated in Figure 4. A plane hexagonal mosaic covering one face of the icosahedron is constructed, using a lattice spacing of  $2S/\sqrt{T'}$ , and the

```

C      To find order of tessellation closest to TREQ
C      All variables are declared as integers
C      NL : lower integer value
C      NU : upper integer value
C      Ti : T value using integer values
C      TREQ : T value required

NL=int(2*SQRT(1/T))/3
NU=2*((NL/2)+1)
DO 2 N=NL,NU
    ht=N/2
    DO 1 h=ht,0,-1
        k=N-h
        Ti=h*h+h*k+k*k
        dT=Ti-TREQ
        IF (dT.LE.0) THEN
            IF (dT.GT.dTb) THEN
                dTb=dT
                dhb=h
                dkb=k
                Tb=Ti
            ENDIF
        ELSEIF (dT.GT.0) THEN
            IF (dT.LT.dTa) THEN
                dTa=dT
                dha=h
                dka=k
                Ta=Ti
                GOTO 3
            ENDIF
        ELSEIF
        ENDIF
1      CONTINUE
2      CONTINUE
3      CONTINUE

```

Figure 3. Fortran-77 algorithm employed to find a desired order of tessellation (TREQ). The values of T are determined that are closest above and below TREQ (respectively  $T_a$  and  $T_b$ ), together with the corresponding values of h and k (respectively, dha, and dka and dhb, dkb)

three vectors **i**, **j**, and **k** (defined in Figure 4a). The points *R* on this grid that are accepted as part of the tessellation on this face, satisfy the criterion:

$$\Delta ABC = \Delta ARC + \Delta ARB + \Delta BRC \quad (2)$$

where *A*, *B*, and *C* are the three vertices of the reference icosahedral face, and  $\Delta$  indicates a triangle area (see Figure 4b). Triangle areas are calculated by Heron's formula:

$$\Delta = (s(s - d_1)(s - d_2)(s - d_3))^{1/2} \quad (3)$$

where  $d_1$ ,  $d_2$ , and  $d_3$  are the lengths of the sides of the triangle and  $2s = d_1 + d_2 + d_3$

- (5) For each point *R* in the tessellation, a set of barycentric coordinates *B* is produced, using the triangle areas calculated above:

$$\begin{aligned} B_1 &= \Delta ARC / \Delta ABC \\ B_2 &= \Delta ARB / \Delta ABC \\ B_3 &= \Delta BRC / \Delta ABC \end{aligned} \quad (4)$$

The tessellation pattern can then be repeated quite con-

veniently over the remaining 19 icosahedral faces, with the Cartesian coordinates of the new points generated as weighted averages of those for the relevant 3 vertices. Thus, for an icosahedron face defined by the vertices  $(x_a, y_a, z_a)$ ,  $(x_b, y_b, z_b)$ , and  $(x_c, y_c, z_c)$ , the tessellation locus with barycentric coordinates  $(B_1, B_2, B_3)$  is obtained as:

$$\begin{aligned} x &= B_1 x_a + B_2 x_b + B_3 x_c \\ y &= B_1 y_a + B_2 y_b + B_3 y_c \\ z &= B_1 z_a + B_2 z_b + B_3 z_c \end{aligned} \quad (5)$$

To avoid duplication of the 12 original icosahedral vertices, all points with barycentric coordinates (1, 0, 0), (0, 1, 0), or (0, 0, 1) are disregarded. In addition, any points that have a single 0 barycentric coordinate, are stored and processed separately, so that there is no duplication of new edge points as the tessellation is repeated over adjacent icosahedral faces.

- (6) The monolayer template is then completed by projecting all vertices onto a sphere of radius  $P$  Å, (see Step 2 above).

The algorithm described here for producing spherical projections of triangularly tessellated icosahedra is general and fully automated. It is superior to other procedures that have been reported, first, because it can cater to *any* allowed order of tessellation (not simply cases where  $T = h^2$  (see Ref. 12) or  $T = 3h$  (see Ref. 13)), and second, because it reproduces the tessellation by means of barycentric coordinates, so that there is no necessity to generate and then eliminate redundant vertices.<sup>12</sup> The same algorithm may also find applications in the modeling of molecular surfaces,<sup>12</sup> the low-resolution structures of virus particles, and atomic clusters.<sup>14</sup>

## Construction of the vesicle bilayer

With the completion of the icosahedral tessellation, a monolayer template is obtained which has sufficient loci to accommodate  $T'$  lipid head groups. The next step in modeling, therefore, is to take  $T'$  copies of the appropriate lipid molecules, placing their head groups at the calculated positions, and arranging their hydrocarbon chains to be oriented along the vectors defined by the center of the vesicle and the tessellation loci. In the case of the outer monolayer of the vesicle, the hydrocarbon chains are directed inward, and for the inner monolayer they are directed outward.

Although it is possible to use VESICA to construct a model for a complete lipid vesicle, for most purposes this is likely to be unnecessary. In its normal use, therefore, the program generates atomic coordinates for just 14 of the bilayer lipids, 7 of these forming a *hexagonal unit* from the outer monolayer (see Color Plate 1) and another 7 forming an equivalent unit from the inner monolayer.

## Modification of the lipid conformation

When the vesicle bilayer segment has been completed, the conformations of the lipid molecules are interactively adjusted so as to be consistent with the bilayer dimensions determined by experiment (*vide infra*). Since the lipids within

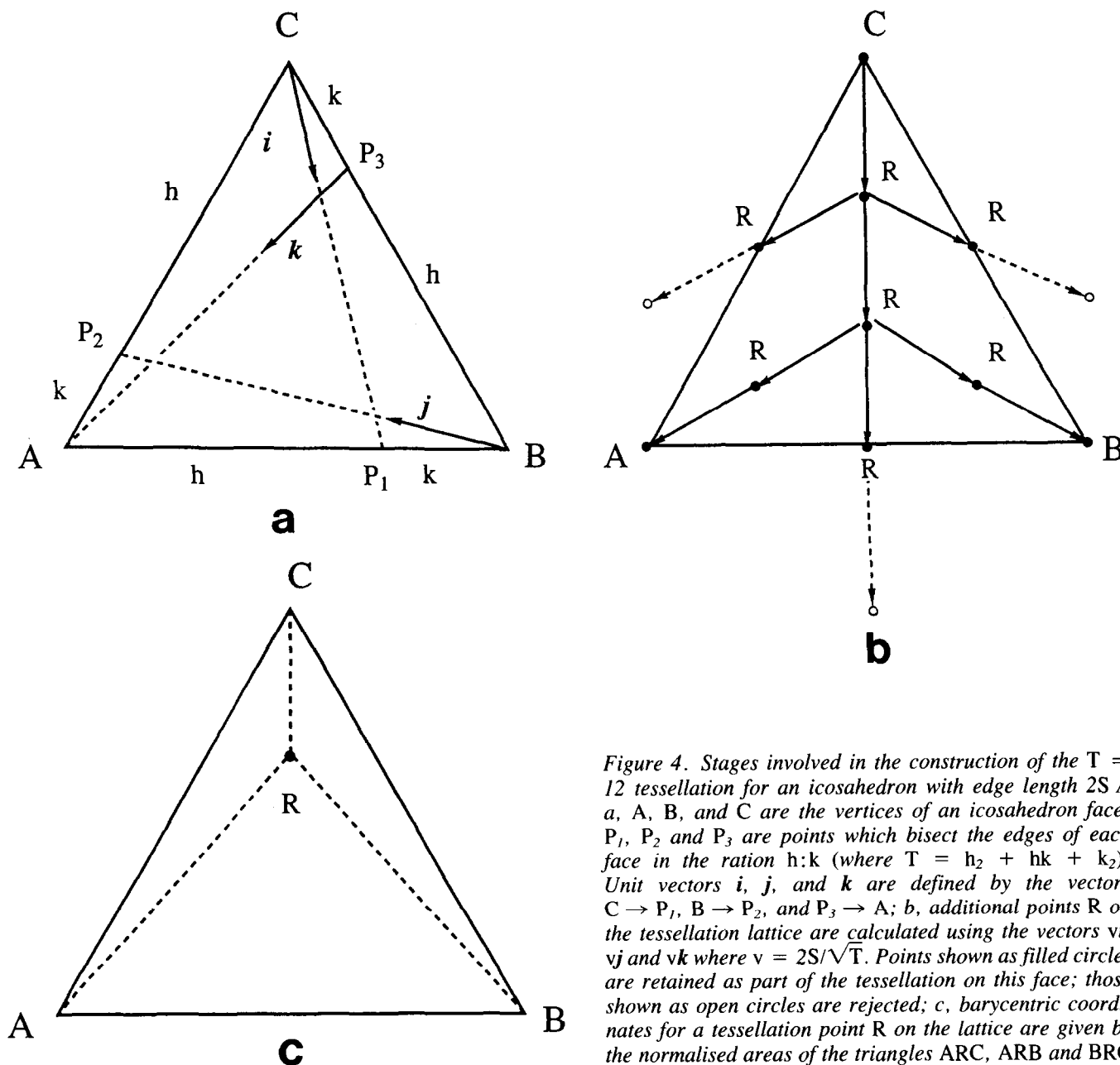


Figure 4. Stages involved in the construction of the  $T = 12$  tessellation for an icosahedron with edge length  $2S \text{ \AA}$ .  $A$ ,  $B$ , and  $C$  are the vertices of an icosahedron face;  $P_1$ ,  $P_2$  and  $P_3$  are points which bisect the edges of each face in the ratio  $h:k$  (where  $T = h_2 + hk + k_2$ ). Unit vectors  $i$ ,  $j$ , and  $k$  are defined by the vectors  $C \rightarrow P_1$ ,  $B \rightarrow P_2$ , and  $P_3 \rightarrow A$ ;  $b$ , additional points  $R$  on the tessellation lattice are calculated using the vectors  $vi$ ,  $vj$  and  $vk$  where  $v = 2S/\sqrt{T}$ . Points shown as filled circles are retained as part of the tessellation on this face; those shown as open circles are rejected;  $c$ , barycentric coordinates for a tessellation point  $R$  on the lattice are given by the normalised areas of the triangles  $ARC$ ,  $ARB$  and  $BRC$

the membrane exist in a fluid-like state,<sup>5</sup> it is important to note here that the model produced should be considered as a time- and space-averaged configuration of the bilayer, rather than as a uniquely defined one.

## RESULTS

In applying VESICA to investigate the relationship between lipid structure and that of the resultant vesicles, we have first studied the well-documented case of SUVs composed of DPPC.

There are two different models that have been proposed for the 3D structure of DPPC SUVs, the first (Model A) due to Huang and Mason,<sup>15</sup> and the second (Model B) due to Cornell et al.<sup>16</sup> The former assumes that the vesicle hydration layer is separate from that of the polar head group

region, and the latter assumes that it is an integral part of this region (see Figure 5).

For both DPPC SUV models, the dimensions of the vesicle and its bilayer (shown in Figure 6) are calculated<sup>16</sup> using the experimentally determined value of the vesicle weight ( $M$ ), the numbers of lipid molecules in the inner and outer monolayers ( $x_i$  and  $x_o$ ), the hydrated vesicle radius ( $R_h$ ), the partial specific volume of DPPC ( $v$ ), and the molecular volume of the phosphatidylcholine head group ( $v_p$ ). Table 1 shows a summary of the data employed, and illustrates the difference between Models A and B.

In the generation of the monolayer templates for the SUV's, the inner vesicle radius,  $R_i$ , is obtained as:

$$R_i = \{R_o^3 - (4 \pi N/3VM)\}^{1/3} \quad (6)$$

where  $N$  is Avogadro's number, and  $R_o$  is the outer vesicle

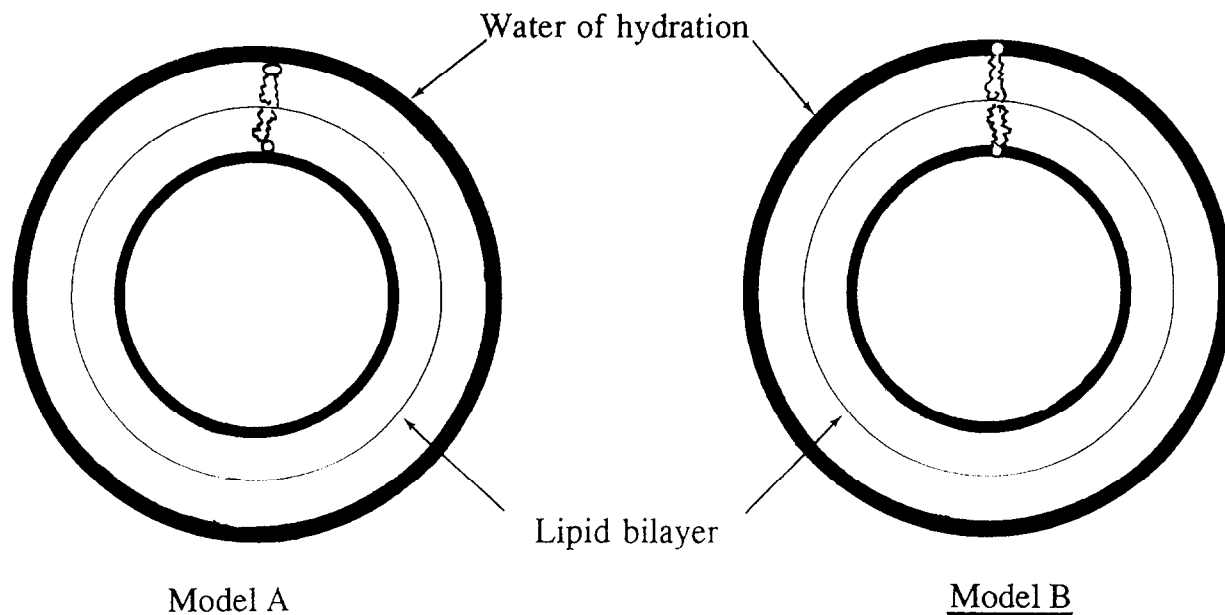


Figure 5. Schematic representations showing cross-sectional views of the alternative models proposed for phospholipid SUVs. Model A assumes<sup>15</sup> that the water of hydration associated with the vesicle is separate from the lipid bilayers; Model B assumes<sup>16</sup> that it forms an integral part of the polar head group region.

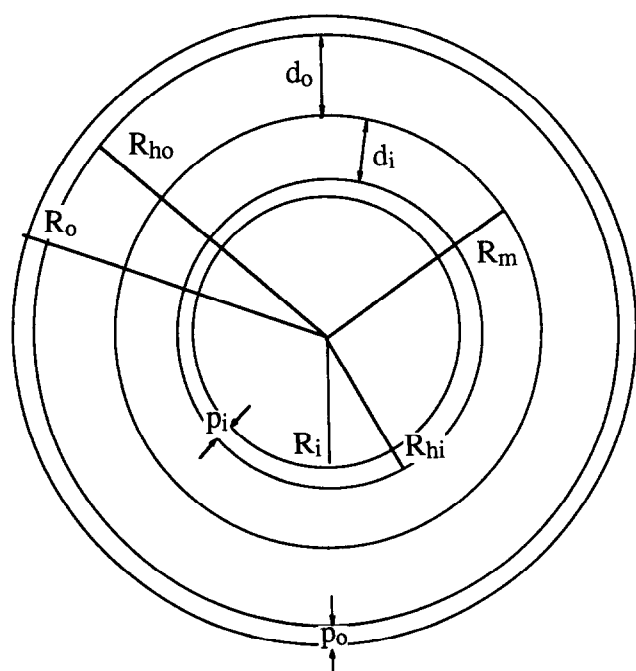


Figure 6. A schematic cross-sectional view of an SUV showing the various vesicle and bilayer dimensions:  $R_o$ , outer radius;  $R_i$ , inner radius;  $R_m$ , monolayer interface radius;  $R_{ho}$ , outer hydrocarbon-water interface radius;  $R_{hi}$ , inner hydrocarbon-water interface radius;  $d_o$ , outer lipid glycerohydrocarbon layer;  $d_i$ , inner lipid glycerohydrocarbon layer;  $p_o$ , outer lipid polar head group layer; and  $p_i$ , inner lipid polar head group layer

radius (calculated from  $R_h$ , Table 1). The radii of the inner and outer hydrocarbon-water interfaces (respectively  $R_{hi}$  and  $R_{ho}$ ) are then found from:

$$x_o v_p = 4 \pi (R_o^3 - R_{ho}^3) / 3; \quad x_i v_p = 4 \pi (R_{hi}^3 - R_i^3) / 3 \quad (7)$$

The monolayer templates are thus produced using  $R_{hi}$  and  $R_{ho}$ , along with the values of  $T$  that give the closest approximations to  $x_i$  and  $x_o$ . (Note that  $R_{hi}$  and  $R_{ho}$  are used in preference to  $R_i$  and  $R_o$  because of ease of identifying the parts of the lipid molecules that would fall at the hydrocarbon-water interface).

A set of seven DPPC molecules is then placed in position on each of the two tessellation lattices (using the reference points illustrated in Figure 7), and the conformations of the lipids are interactively adjusted so that their head groups and glycerohydrocarbon regions are confined within the appropriate (calculated) thicknesses of the bilayer.

The thickness of the glycerohydrocarbon regions ( $d_o$  and  $d_i$ ) are calculated as:

$$d_o = R_{ho} - R_m; \quad d_i = R_m - R_{hi} \quad (8)$$

where  $R_m$  is the radius of the intermonolayer boundary, given by:

$$R_m = [(R_o^3 x_i + R_i^3 x_o) / (x_o + x_i)]^{1/3} \quad (9)$$

The thickness of the phosphatidylcholine regions ( $p_o$  and  $p_i$ ) are obtained simply as:

$$p_o = R_o - R_{ho}; \quad p_i = R_{hi} - R_i \quad (10)$$

The values of the various dimensions so obtained for Models A and B are listed in Table 2.

**Table 1. Experimental data employed in calculating the bilayer dimensions for DPPC SUV Models A<sup>15</sup> and B.<sup>16</sup> For Model A, the outer vesicle radius is obtained as  $R_h - 6 \text{ \AA}$ , to account for a separate hydration layer; for Model B,  $R_o$  is taken as  $R_h$ , since the hydration layer is considered part of the outer lipid polar head group layer. The value of  $M$  quoted for Model B represents the weight of the hydrated vesicles determined by experiment; the value quoted for Model A represents the experimental vesicle weight minus the weight of associated water molecules**

Parameter		Model A	Model B
Hydrated SUV radius	$(R_h, \text{\AA})$		105
Outer SUV radius	$(R_o, \text{\AA})$	99	105
SUV weight	$(M, kD)$	1880	2430
Number of inner/outer lipid	$(x_i/x_o)$		790/1658
Partial specific volume of DPPC	$(v, \text{g/ml})$	0.9848	0.9882
Mol. volume of PC head group	$(v_p, \text{\AA}^3)$	205	573.8

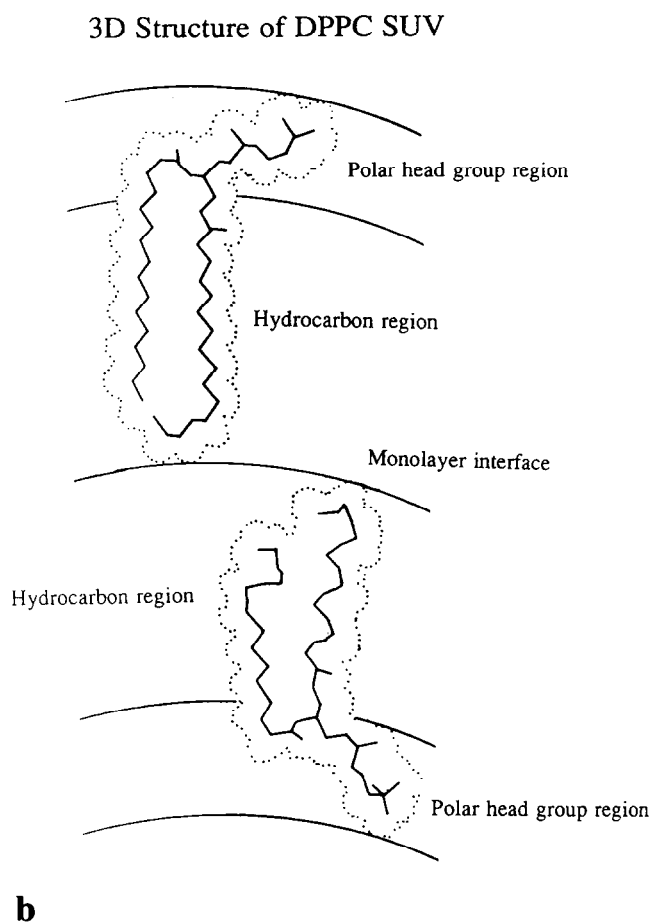
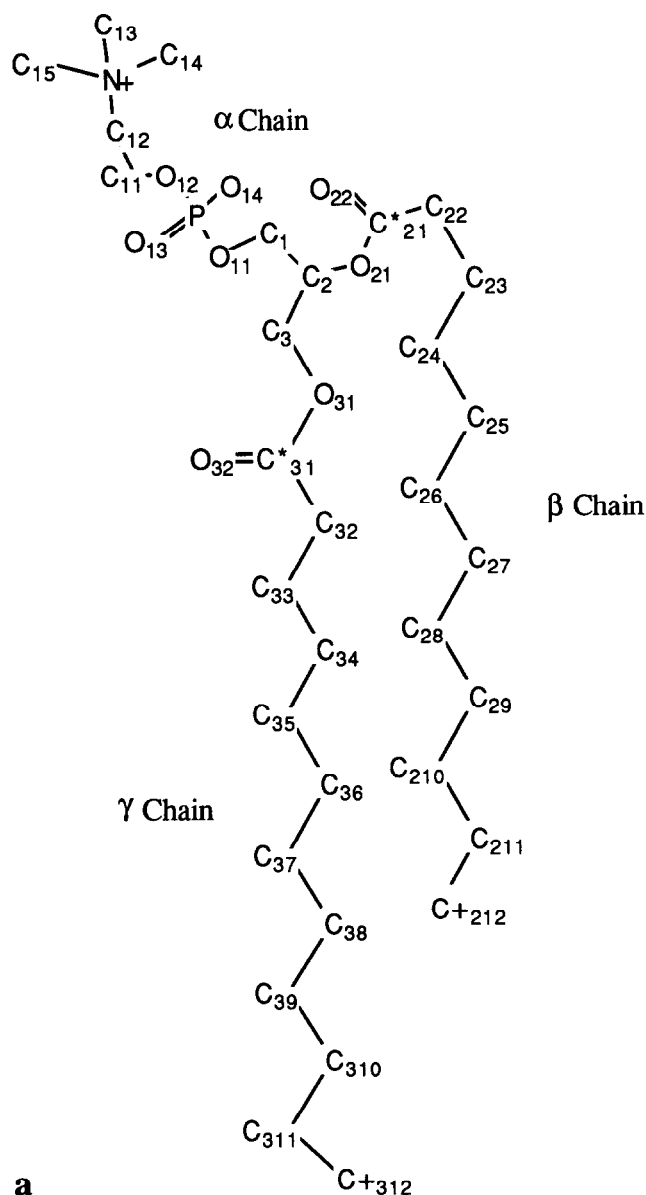


**Figure 7. a, DPPC structure showing the atoms (marked by \*) that are used to define the centroid of the lipid interface region, and the atoms (marked by +) that are used to orientate the alkyl chains with respect to the SUV center. Numbering convention as used in Schuh et al.<sup>17</sup> b, representative conformations of the lipids in the outer and inner monolayers of a DPPC SUV modeling according to the data of Cornell et al.<sup>16</sup>**

**Table 2. DPPC SUV dimensions determined according to the assumptions of Huang and Mason (Model A)<sup>15</sup> and Cornell et al. (Model B).<sup>16</sup> Symbols used are as defined in Figure 6, with radii and distances expressed in Å, and areas in Å<sup>2</sup>;  $a_{ho}$  and  $a_{hi}$  are the interfacial areas per lipid molecule calculated at  $R_{ho}$  and  $R_{hi}$ , respectively.**

Lipid Parameter		Model A	Model B
Outer radius	( $R_o$ )	99.0	105.0
Monolayer interface radius	( $R_m$ )	78.0	80.1
Inner radius	( $R_i$ )	61.8	59.2
Outer lipid–water interface radius	( $R_{ho}$ )	96.2	97.6
Inner lipid–water interface radius	( $R_{hi}$ )	65.0	68.1
Outer lipid area/molecule	( $a_{ho}$ )	70.1	72.2
Inner lipid area/molecule	( $a_{hi}$ )	67.2	73.7
Outer lipid glycerohydrocarbon layer	( $d_o$ )	21.1	17.5
Inner lipid glycerohydrocarbon layer	( $d_i$ )	16.1	12.0
Outer lipid head group layer	( $p_o$ )	2.8	7.4
Inner lipid head group layer	( $p_i$ )	3.2	8.9

For Model A, it is found that both the inner and outer lipid alkyl chains can be readily accommodated in the allotted space of the bilayer, simply by introducing coiling. With the outer, and more particularly, the inner lipid head groups, however, it proves impossible to find stereochemically acceptable conformations that alleviate the close contacts between neighboring molecules. In addition, it is noted that there are quite different interfacial areas per molecule for the two monolayers in this model, which is intuitively unsatisfactory.

Model B, on the other hand, produces a perfectly acceptable bilayer structure, in which the areas per molecule in the two monolayers are roughly equal, and the hydrophilic and hydrophobic portions of the two sets of lipids are fitted easily within their allotted regions. In this model, the outer lipid conformation is adjusted to move the  $\alpha$ -chain down towards the vesicle surface (by rotation about the  $C_1-O_{11}$  bond, see Figure 7), and the inner lipid conformation is adjusted (in a similar way) so as to incline the head group towards the SUV centre. The inner lipid  $\gamma$ -chains are coiled significantly and those of the outer lipids are 80% extended.

*Note:* To assess the influence of errors in the experimental measurements used in these modeling calculations, it is sufficient to consider only the most critical parameters, viz., the number of lipid molecules within each of the monolayers. By experiment, the number of lipid molecules are calculated as 1658 (in the outer monolayer) and 790 (in the inner monolayer). The corresponding values used by VESICA are 1632 and 792. These differences translate to an error of  $\sim 1\%$  in the vesicle weight (1.90 kD versus 1.88 kD), and so are well within experimental error, estimated to be at worst 10%.<sup>15</sup> We therefore believe that experimental errors are unlikely to cause sufficient changes of bilayer dimensions to discredit any conclusions obtained from models generated by VESICA.

## DISCUSSION

In the application of VESICA to discriminate between alternative models proposed for the 3D structure of DPPC

SUVs, the simulations show that the more realistic model is obtained following the assumption of Cornell et al., that the vesicle hydration layer is integral to the polar head group region.<sup>16</sup> The simulation based on the original data of Huang and Mason<sup>15</sup> leads to a bilayer structure in which there is unacceptable and unavoidable overlap between the lipid polar head groups.

In future studies the feasibility and relative stabilities of the two vesicle structures may be checked by carrying out simple molecular mechanics calculations. For the present, however, we would simply note that there is additional support for the model due to Cornell et al., in that the predicted differences in the conformations of the inner and outer lipid head groups, are consistent with the data obtained in NMR studies.<sup>17,18</sup> The molecular graphics work shows the outer lipid conformation to be most similar to that seen in the DPPC crystal.<sup>19</sup>

Analysis of the model produced according to Cornell et al. also shows that the inner lipid  $\gamma$ -chains can only be accommodated in the bilayer if they are coiled to around 60% of their extended length. Since any further degree of coiling is stereochemically impossible, this suggests that the lipid alkyl chain length may be an important factor in determining the minimum vesicle size. Related studies<sup>9</sup> on other lipids within the series confirm this observation, and suggest that the minimum vesicle size will also be limited by the nature of the (inner) lipid head group. Taken together these studies indicate that the minimum size of an SUV is not limited simply by chain packing in the hydrocarbon region,<sup>20</sup> or by the inner polar head group interactions,<sup>16</sup> but by a combination of both factors.

## CONCLUSION

A computer program VESICA has been developed that allows for molecular graphics modeling of the 3D structures of lipid vesicles. The program has been successfully employed in analyzing the molecular architecture of phospholipid SUVs, and may be readily adapted to generate 3D models for spherical micelles, inverted micelles and micro-

emulsions. In future work, the program will be used to study aggregates of lipid mixtures (including lipid-drug systems) and ultimately will be employed as an aid in the design of lipid-based drug delivery vehicles.

## ACKNOWLEDGEMENTS

S. M. Lawrence gratefully acknowledges the receipt of an SERC Earmarked Chemistry Committee Award, and DJB, a University of London Central Research Fund grant.

## REFERENCES

- 1 Bangham, A.D., Hill, M.W., and Miller, N.G.A. Preparation and use of liposomes as models of biological membranes. *Meth. Membrane Biol.* 1974, **1**, 1-68
- 2 Ostro, M.J. *Liposomes: From Biophysics to Therapeutics*. M. Dekker Inc., New York, 1988
- 3 Illum, L. and Davis, S.S. The organ uptake of intravenously administered colloidal particles can be altered using nonionic surfactant (Poloxamer 388). *FEBS Lett.* 1984, **167**, 79-82
- 4 Chauhan, S. and Lawrence, M.J. The properties of polyoxyethylene containing nonionic surfactant vesicles. *J. Pharm. Pharmacol.* 1989, **41**, (supp.), 6P
- 5 Tanford, C. *The Hydrophobic Effect*. John Wiley & Sons, New York, 1973
- 6 Israelachvili, J.N., Mitchell, D.J., and Ninham, B.W. Theory of self-assembly of hydrocarbon amphiphiles into micelles and bilayers. *J. Chem. Soc., Faraday Trans. II*, 1976, **72**, 1525-1568
- 7 Gaber, B.P., Light, W.R., and Brown, R.M. Molecular graphics of lipid structures. *J. Mol. Graphics*, 1988, **6**, 212-213
- 8 Lawrence, S.M., Lawrence, M.J., and Barlow, D.J. Computer simulation of lipid assemblies. *Biochem. Soc. Trans.* 1990, **18**, 943
- 9 Lawrence, S.M., Lawrence, M.J., and Barlow, D.J. Molecular architecture of phosphatidylcholine small unilamellar vesicles (PC SUVs). *J. Pharm. Pharmacol.* 1990, **42** (supp.), 49P
- 10 Small, D.M. Lateral chain packing in lipids and membranes. *J. Lipid Res.* 1984, **25**, 1490-1499
- 11 Barret, A.N. and Mackay, A.L. In: *Spatial structure and the microcomputer*. Macmillan, Basingstoke, 1987, pp 343-392
- 12 Chau, P.L. and Dean, P.M. Molecular recognition: 3D surface structure comparison by gnomonic projection. *J. Mol. Graphics*, 1987, **5**, 97-100
- 13 Kabsch, W. and Sander, C. Dictionary of protein secondary structure: Pattern recognition of hydrogen-bonded and geometrical features. *Biopolymers* 1983, **22**, 2577-2637
- 14 Mackay, A.L. Carbon crystals wrapped up. *Nature* 1990, **347**, 336-337
- 15 Huang, C. and Mason, J.T. Geometric constraints in egg phosphatidylcholine vesicles. *Proc. Nat. Acad. Sci. USA* 1978, **75**, 308-310
- 16 Cornell, B.A. Middlehurst, J., and Separovic, F. The molecular packing and stability within highly curved phospholipid bilayers. *Biochim. Biophys. Acta* 1980, **598**, 405-410
- 17 Schuh, J.R., Banerjee, U., Muller, L., and Chan, S.I. The phospholipid packing arrangement in small bilayer vesicles as revealed by proton magnetic resonance studies at 500 MHz. *Biochim. Biophys. Acta* 1982, **687**, 219-225
- 18 Brouillette, C.G., Segret, J.P., Ng, T.C., and Jones, J.L. Minimal size phosphatidylcholine vesicles: Effects of radius of curvature on head group packing and conformation. *Biochemistry* 1982, **21**, 4569-4575
- 19 Hauser, H., Pascher, I., Pearson, R.H., and Sundell, S. Preferred conformation and molecular packing of phosphatidylethanolamine and phosphatidylcholine. *Biochim. Biophys. Acta* 1981, **650**, 21-51
- 20 Israelachvili, J.N., Mitchell, D.J., and Ninham, B.W. Theory of self-assembly of lipid bilayers and vesicles. *Biochim. Biophys. Acta* 1977, **470**, 185-201